Two Methods for Target Localization in Multistatic Passive Radar

MATEUSZ MALANOWSKI, Member, IEEE
KRZYSZTOF KULPA, Senior Member, IEEE
Warsaw University of Technology

This paper compares two algorithms for three-dimensional target localization from passive radar measurements. The algorithms use bistatic range measurements from multiple transmitter-receiver pairs to calculate the target position. The algorithms derived are based on the methods known for time-difference-of-arrival (TDOA) systems, namely spherical interpolation (SI) and spherical intersection (SX). Both algorithms rely on closed-form equations. A theoretical accuracy analysis of the algorithms is provided. This analysis is verified with Monte-Carlo simulations and a real-life example is presented.

Manuscript received March 31, 2010; revised October 21, 2010; released for publication January 26, 2011.

IEEE Log No. T-AES/48/1/943634.

Refereeing of this contribution was handled by S. Coraluppi.

This work was supported by the European Union in the framework of the European Social Fund through the Warsaw University of Technology Development Program.

Authors' address: Institute of Electronic Systems, Warsaw University of Technology, Nowowiejska 15/19, Warsaw, Poland, E-mail: (m.malanowski@elka.pw.edu.pl).

I. INTRODUCTION

This paper deals with a problem of target localization based on measurements from passive radar. Passive radar, also known as passive coherent location (PCL) radar, passive bistatic radar (PBR), or passive covert radar (PCR), uses existing transmitters as illuminators of opportunity [4, 9, 3, 14, 7]. By comparing the reference signal with an echo reflected from a target, the relative delay can be measured. The delay is related to the bistatic range, which is the sum of transmitter-target and target-receiver ranges. The locus of points of constant bistatic range is an ellipsoid with foci located at the transmitter and receiver positions. If bistatic measurements corresponding to multiple transmitter-receiver pairs are available, the target position can be calculated as the intersection of different ellipsoids. To localize a target unambiguously in three-dimensional space, at least three ellipsoids are required.

The problem of localization in passive radar is related to hyperbolic positioning, where a position is calculated by measuring time differences of arrival (TDOA). In this case, the locus of points of constant TDOA defines a hyperbola, when a two-dimensional situation is considered, or a hyperboloid in three-dimensional space. Localizing the target consists in finding the intersection of the hyperbolas (or hyperboloids).

Both localization problems, in passive radar as well as in a TDOA system, are potentially challenging due to the nonlinear relationships between the desired target position and measured parameters (bistatic ranges or TDOAs). Several solutions using simple closed-form equations have been proposed for TDOA systems [11, 10, 13, 1, 8].

In open literature, an analytic solution for finding the intersection points of bistatic range ellipsoids in three-dimensional Cartesian space has not been found. As a result, the authors of this paper have decided to derive their own analytic methods for localization in passive radars based on two established approaches to TDOA localization, namely spherical-interpolation (SI) method [10, 1] and spherical-intersection (SX) method [13, 8]. The two algorithms proposed for passive radar are shown to differ from known TDOA solutions in sign only. The methods are compared from the viewpoint of their accuracy. This paper is an extension of our work presented in [5].

The problem of target localization considered in this paper is a static one, i.e., given the bistatic measurements at a specific point in time, the target position is calculated. Another consideration is the problem of combining the process of localization with the tracking algorithm. This can be achieved in several ways. For example, bistatic trackers can be used for each of the transmitters separately followed by the localization algorithm, or the localization on

raw bistatic data can be followed by a Cartesian tracker. This problem is, however, outside the scope of this paper. The problem of target tracking in multistatic passive radar is addressed in [15] and [2]. Regardless of the tracker used, the localization algorithms proposed in this paper are deemed to be important, an example of this being their use in the initialization of the Cartesian tracks.

We consider a situation with only one target. In reality, multiple targets may be observed, which can lead to a ghost target phenomenon. This occurs when the ellipsoids corresponding to different targets intersect in a way that gives rise to a spurious target. The ambiguity in the association of the bistatic measurements to the targets has to be resolved. This can be facilitated with a tracking algorithm through analyzing the history of the measurements—if they are not consistent, the target is deemed false. The need to solve such ambiguities does not render the presented algorithms useless; on the contrary, they can be used to calculate candidate target position estimates by considering all possible combinations of the measurements. Since the number of possibilities grows exponentially with the number of targets, additional emphasis is put on the speed of the algorithm for calculating position estimates.

The paper is organized as follows. Section II formulates the problem of target localization in multistatic passive radar. The two algorithms are derived in Section III. In the same section, the analysis of the theoretical accuracy is carried out. Section IV is devoted to the numerical results obtained by processing simulated and real-life data. The paper ends with conclusions in Section V.

II. PROBLEM FORMULATION

Consider the system geometry shown in Fig. 1. Here we deal with one receiver and multiple transmitters; however, the situation with multiple receivers and a single transmitter is equivalent. Without loss of generality we assume that the receiver is located at position $[0,0,0]^T$. The number of transmitters N is arbitrary, but not lower than three. The ith transmitter is located at position $[x_i, y_i, z_i]^T$ for $i = 1,\ldots,N$, and the target is located at coordinates $\mathbf{x}_t = [x_t, y_t, z_t]^T$ (we assume a point scatterer target). We focus on the estimation of the position of the target only; therefore, the target velocity is not taken into account. The distance between the target and the receiver is

$$R_t = \sqrt{x_t^2 + y_t^2 + z_t^2} = \|\mathbf{x}_t\| \tag{1}$$

where $\|\mathbf{x}\| = \sqrt{\mathbf{x}^T\mathbf{x}}$ is the norm of the vector. The distance between the target and the ith transmitter is

$$\begin{aligned} R_{ti} &= \sqrt{(x_i - x_t)^2 + (y_i - y_t)^2 + (z_i - z_t)^2} \\ &= \|\mathbf{x}_i - \mathbf{x}_t\| \end{aligned} \tag{2}$$

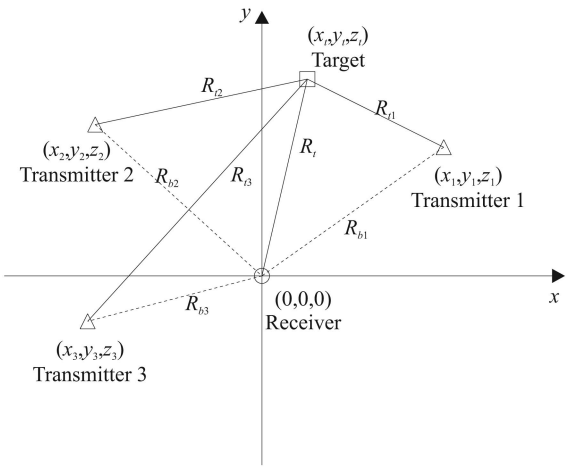

Fig. 1. Geometry of target localization in passive radar (for 3 transmitters).

and the base range corresponding to the ith transmitter can be calculated as

$$R_{bi} = \sqrt{x_i^2 + y_i^2 + z_i^2} = \|\mathbf{x}_i\|. \tag{3}$$

In passive radar, a crossambiguity function is calculated between the reference signal and the surveillance signal (containing target echoes) [4]. Calculation of the crossambiguity function consists in correlating the two signals with appropriate delay and frequency shift. If the delay and frequency shift of the reference signal match those of the target echo, a correlation peak appears. From the position of the peak, the values of the TDOA[1] and Doppler shift can be calculated. The TDOA multiplied by the speed of light is the range difference between the direct and indirect paths. In the passive radar community, this range difference is usually called bistatic range. However, for the purpose of this paper, we define the bistatic range as the sum of transmitter-target range R_{ti} and target-receiver range R_t. According to this definition, the bistatic range is the range difference measured by passive radar plus the base range R_{bi}

$$\begin{aligned} R_i &= (R_{ti} + R_t - R_{bi}) + R_{bi} = R_{ti} + R_t \\ &= \sqrt{(x_i - x_t)^2 + (y_i - y_t)^2 + (z_i - z_t)^2} + \sqrt{x_t^2 + y_t^2 + z_t^2}. \end{aligned} \tag{4}$$

The vector of the bistatic ranges corresponding to N transmitters is denoted as

$$\mathbf{r} = \begin{bmatrix} R_1 \\ R_2 \\ \vdots \\ R_N \end{bmatrix}_{N\times 1}. \tag{5}$$

[1]In this context, TDOA is calculated as the difference between the transmitter-target-receiver and transmitter-receiver paths. This is something different than in TDOA systems, where time differences between signal transmission from a single source and signal reception by different receivers are considered.

Define a vector of bistatic ranges $\hat{\mathbf{r}}(\hat{\mathbf{x}}_t) = [\hat{R}_1, \hat{R}_2, \ldots, \hat{R}_N]^T$ calculated for an assumed position estimate $\hat{\mathbf{x}}_t = [\hat{x}_t, \hat{y}_t, \hat{z}_t]^T$ using (4). Our aim is to find the target position estimate $\hat{\mathbf{x}}_t$ that minimizes the norm of the error between the vector of measured bistatic ranges $\mathbf{r}$ and the vector of bistatic ranges $\hat{\mathbf{r}}(\hat{\mathbf{x}}_t)$ corresponding to the estimated position $\hat{\mathbf{x}}_t$:

$$\hat{\mathbf{x}}_t = \arg\min_{\hat{\mathbf{x}}_t} \|\mathbf{r} - \hat{\mathbf{r}}(\hat{\mathbf{x}}_t)\|. \tag{6}$$

The above optimization problem is difficult to solve due to the nonlinear relationship between the target position and its bistatic parameters. The cost function (norm of the error) may have local minima. Therefore, the application of standard numerical optimization methods may not give the correct result if the starting point is chosen incorrectly. Moreover, iterative optimization methods are usually time consuming, so a simple closed-form solution is preferred if one can be found.

III. THE ALGORITHM

A. Position Estimation

We show that it is possible to find an estimate of the target position by closed-form equations that approximately satisfy (6). This can be achieved by rearranging (4) in the following way:

$$R_i - \sqrt{x_t^2 + y_t^2 + z_t^2} = \sqrt{(x_i - x_t)^2 + (y_i - y_t)^2 + (z_i - z_t)^2}. \tag{7}$$

By squaring both sides and rearranging the terms, we obtain

$$x_i x_t + y_i y_t + z_i z_t - R_i \sqrt{x_t^2 + y_t^2 + z_t^2} = \tfrac{1}{2}(x_i^2 + y_i^2 + z_i^2 - R_i^2). \tag{8}$$

To simplify notation, we introduce a matrix of transmitter positions

$$\mathbf{S} = \begin{bmatrix} x_1 & y_1 & z_1 \\ x_2 & y_2 & z_2 \\ \vdots & \vdots & \vdots \\ x_N & y_N & z_N \end{bmatrix}_{N\times 3} \tag{9}$$

and an additional vector defined as

$$\mathbf{z} = \frac{1}{2}\begin{bmatrix} x_1^2 + y_1^2 + z_1^2 - R_1^2 \\ x_2^2 + y_2^2 + z_2^2 - R_2^2 \\ \vdots \\ x_N^2 + y_N^2 + z_N^2 - R_N^2 \end{bmatrix}_{N\times 1}. \tag{10}$$

With the above notation, (8) can be written for N transmitters in a matrix form:

$$\mathbf{S}\mathbf{x}_t = \mathbf{z} + \mathbf{r}R_t. \tag{11}$$

The unknowns in this equation are the target position $\mathbf{x}_t$ and the target-receiver range R_t. The above equation is linear in $\mathbf{x}_t$ as well as in R_t. Assuming that R_t is known, the solution in the least squares sense can be found as

$$\hat{\mathbf{x}}_t = (\mathbf{S}^T\mathbf{S})^{-1}\mathbf{S}^T\mathbf{z} + (\mathbf{S}^T\mathbf{S})^{-1}\mathbf{S}^T\mathbf{r}R_t. \tag{12}$$

Before calculating (12), however, the value of R_t has to be found.

In the literature, two methods for calculating R_t can be found in the context of TDOA localization: SI [13, 1] and SX [10, 8]. In SI, R_t is calculated from a certain quotient, while in SX, R_t is obtained from a quadratic equation. These algorithms were compared in [12], which showed that the SX method is much more robust to measurement errors in the case of a TDOA system.

We derive two analogous algorithms for the passive radar case and compare them in Section IV. We show that for the analyzed passive radar scenario the SI method provides better results than SX.

Before considering the two methods for calculating R_t, it is worth mentioning that (12) is not the solution of the original problem (6), but a different problem resulting from a rearrangement of the equations. However, those two problems are closely related. In the case of lack of measurement errors, they both lead to the same results. In a realistic scenario, when measurement errors are present, the proposed approach also leads to satisfactory results, which is shown later in the paper.

B. Spherical-Interpolation Method

Equation (12) can be compactly written as

$$\hat{\mathbf{x}}_t = \mathbf{S}^*(\mathbf{z} + \mathbf{r}R_t) \tag{13}$$

where $\mathbf{S}^* = (\mathbf{S}^T\mathbf{S})^{-1}\mathbf{S}^T$. The above equation can be used to compute the equation error $\boldsymbol{\epsilon}$, which is the difference of the right-hand and left-hand sides of (11):

$$\boldsymbol{\epsilon} = \mathbf{z} + \mathbf{r}R_t - \mathbf{S}\mathbf{S}^*(\mathbf{z} + \mathbf{r}R_t) = (\mathbf{I} - \mathbf{S}\mathbf{S}^*)(\mathbf{z} + \mathbf{r}R_t). \tag{14}$$

In this way, we eliminated the unknown $\hat{\mathbf{x}}_t$. We introduce a matrix

$$\mathbf{T} = \mathbf{I} - \mathbf{S}\mathbf{S}^*. \tag{15}$$

This matrix is idempotent, i.e., $\mathbf{T}^2 = \mathbf{T}$, and it is symmetrical, i.e., $\mathbf{T} = \mathbf{T}^T$. Using these properties, R_t can be calculated by minimizing the norm of the error (14) $\|\boldsymbol{\epsilon}\|$ as

$$\hat{R}_t = -\frac{\mathbf{r}^T\mathbf{T}\mathbf{z}}{\mathbf{r}^T\mathbf{T}\mathbf{r}}. \tag{16}$$

In this method, the condition $\hat{R}_t = \|\hat{\mathbf{x}}_t\|$ has not been enforced anywhere; in general, $\hat{R}_t$ calculated from (16) and $\|\hat{\mathbf{x}}_t\|$ will differ. To obtain the target position estimate $\hat{\mathbf{x}}_t$, the value of $\hat{R}_t$ calculated from (16) is substituted into (12) or (13).

The SI method cannot be used in the case of a minimal number of transmitters (3 in the considered case), since the residual ϵ in (14) would equal 0.

C. Spherical-Intersection Method

The second method for calculating R_t is based on the SI method [10, 8]. Unlike the method in the previous subsection, it can be used with a minimal number of transmitters (3 in the considered case). The derivation of this method is as follows. First, new variables are introduced:

$$\mathbf{a} = (\mathbf{S}^T\mathbf{S})^{-1}\mathbf{S}^T\mathbf{z} \tag{17}$$

and

$$\mathbf{b} = (\mathbf{S}^T\mathbf{S})^{-1}\mathbf{S}^T\mathbf{r}. \tag{18}$$

With this notation, (11) can be written as

$$\mathbf{x}_t = \mathbf{a} + \mathbf{b}R_t. \tag{19}$$

Now, by substituting $\mathbf{x}_t^T\mathbf{x}_t = \|\mathbf{x}_t\|^2$, inserting the above equation into (1), and squaring both sides, we eliminate $\mathbf{x}_t$ and obtain a quadratic equation in R_t:

$$(\mathbf{b}^T\mathbf{b} - 1)R_t^2 + 2\mathbf{a}^T\mathbf{b}R_t + \mathbf{a}^T\mathbf{a} = 0. \tag{20}$$

The solution of this equation is

$$\hat{R}_t = \frac{-2\mathbf{a}^T\mathbf{b} \mp \sqrt{4(\mathbf{a}^T\mathbf{b})^2 - 4(\mathbf{b}^T\mathbf{b} - 1)\mathbf{a}^T\mathbf{a}}}{2(\mathbf{b}^T\mathbf{b} - 1)}. \tag{21}$$

When $\hat{R}_t$ is found, it can be substituted into (12) to find the position estimate $\hat{\mathbf{x}}_t$.

If the discriminant of (20) is larger than 0, two real-valued solutions for $\hat{R}_t$ exist. In a typical situation, the transmitters are placed close to the x-y plane, so the geometry is almost symmetrical with respect to this plane. Usually, the two values of $\hat{R}_t$ are similar and correspond to the true target and its mirror reflection with respect to the x-y plane. The correct position estimate can be chosen by considering the height of the estimate. Since most applications of passive radar involve flying objects, the position estimate with positive height can be selected; this simple approach is used in this paper. However, one has to be aware that this may not always be the best approach. An example of this is in the detection of very low-flying targets, or operating in an area with a depression. The selection of a solution can be facilitated in the case where more than the minimal number of transmitters are available (at least 4). In such cases, one could compute the error norm of both solutions to (20) and choose the one with the lowest error.

It may also happen that, due to the measurement errors, the discriminant of the quadratic equation (20) is less than 0, so there is no real-valued solution for $\hat{R}_t$. Our experiments have shown that even in such situations, an acceptable solution can still be found. If the discriminant is less than zero, (20) has two complex solutions which are a conjugate pair. Taking the real part of this result and substituting it into (12) still yields a valid position estimate. A drawback of this approach is that the algorithm is deprived of the possibility of rejecting bistatic measurements that are not consistent—every combination of the bistatic measurements will yield a result. This can be disadvantageous from the point of view of the ghost target phenomenon.

The two algorithms for passive radar differ from their TDOA counterparts in sign only [12]. The reason for this is that here we deal with sums of ranges instead of differences.

D. Estimation Accuracy

It is desirable to know the accuracy of the estimated target position, for example, in order to properly initialize the covariance matrix in a tracking filter. Usually, the accuracy of the measurement of the bistatic parameters is known (it can be estimated from the size of the range resolution cell and the signal-to-noise ratio). Our aim is to calculate the accuracy of the position estimate in Cartesian coordinates based on the known accuracy of the bistatic parameters. Denote the variance of the bistatic range error corresponding to the ith transmitter as σ_{Ri}^2. The covariance matrix $\mathbf{R}$ of the measurement error of the bistatic parameters is given by

$$\mathbf{R}_{N\times N} = E[\mathbf{r}\mathbf{r}^T] = \mathrm{diag}\Big(\underbrace{[\sigma_{R1}^2, \ldots, \sigma_{RN}^2]}\Big). \tag{22}$$

The notation above means that $\mathbf{R}$ is a diagonal matrix created from the N-element vector of variances corresponding to N transmitters.

Since the relationship between the target position and its bistatic parameters is nonlinear, it is impossible to give a straightforward expression for the covariance matrix of the position estimate; however, approximate formulae can be obtained. Here we follow the analysis carried out in [13]. Using a first-order Taylor series expansion, the covariance matrix of the position estimate can be approximated as

$$\mathbf{P}_{3\times 3} = E[\hat{\mathbf{x}}_t\hat{\mathbf{x}}_t^T] \approx \left(\frac{\partial \mathbf{x}_t}{\partial \mathbf{r}}\right)\mathbf{R}\left(\frac{\partial \mathbf{x}_t}{\partial \mathbf{r}}\right)^T \tag{23}$$

where $(\partial\mathbf{x}_t/\partial\mathbf{r})_{3\times N}$ is the Jacobian. To calculate the Jacobian, differentiate (11) with respect to $\mathbf{r}$:

$$\mathbf{S}\frac{\partial \mathbf{x}_t}{\partial \mathbf{r}} = \frac{\partial \mathbf{z}}{\partial \mathbf{r}} + \frac{\partial(\mathbf{r}R_t)}{\partial \mathbf{r}}. \tag{24}$$

The first component on the right-hand side of the above equation can be easily calculated as

$$\frac{\partial \mathbf{z}}{\partial \mathbf{r}} = -\begin{bmatrix} R_1 & & & 0 \\ & R_2 & & \\ & & \ddots & \\ 0 & & & R_N \end{bmatrix}_{N\times N} = -\mathbf{\Lambda}. \tag{25}$$

TABLE I
Relative Positions of the Transmitters used for Comparison of the Algorithms

Transmitter	x-offset (km)	y-offset (km)	z-offset (km)
Tx1	20.00	0.00	0.00
Tx2	−30.00	5.00	0.15
Tx3	−10.00	−15.00	0.10
Tx4	10.00	−25.00	0.05

Next we calculate the derivative of the second component of the right-hand side of (24):

$$\frac{\partial(\mathbf{r}R_t)}{\partial\mathbf{r}} = \mathbf{I}R_t + \mathbf{r}\frac{\partial R_t}{\partial\mathbf{r}} \tag{26}$$

where $\mathbf{I}$ is the identity matrix. To calculate $\partial R_t/\partial\mathbf{r}$, we use the chain rule:

$$\frac{\partial R_t}{\partial\mathbf{r}} = \frac{\partial R_t}{\partial\mathbf{x}_t}\frac{\partial\mathbf{x}_t}{\partial\mathbf{r}} = \frac{\mathbf{x}_t^T}{\|\mathbf{x}_t\|}\frac{\partial\mathbf{x}_t}{\partial\mathbf{r}}. \tag{27}$$

Substituting (25) and (26) into (24) yields

$$\mathbf{S}\frac{\partial\mathbf{x}_t}{\partial\mathbf{r}} = -\mathbf{\Lambda} + \mathbf{I}R_t + \mathbf{r}\frac{\mathbf{x}_t^T}{\|\mathbf{x}_t\|}\frac{\partial\mathbf{x}_t}{\partial\mathbf{r}}. \tag{28}$$

By rearranging the above equation, we can express the Jacobian matrix as

$$\frac{\partial\mathbf{x}_t}{\partial\mathbf{r}} = (\Delta^T\Delta)^{-1}\Delta^T(\mathbf{I}R_t - \mathbf{\Lambda}) \tag{29}$$

where

$$\Delta = \mathbf{S} - \mathbf{r}\frac{\mathbf{x}_t^T}{\|\mathbf{x}_t\|}. \tag{30}$$

The covariance matrix of the position estimate can now be calculated using (23). The values on the diagonal of $\mathbf{P}_{3\times3}$ correspond to the variances of the position error in the x, y, and z directions.

In the above considerations only the variance of the estimation error is taken into account. As the analyzed problem is highly nonlinear, the nonlinearity and estimation bias can lead to divergence of the theoretical and practical results. However, analysis of the variance of the estimator often illustrates useful trends even when compared against biased estimators. In the next section we show that in most cases simulation and theoretical analysis are consistent. However for altitude estimation, where it is necessary to select one of the possible solutions of the quadratic equation, results from simulations differ from the theory.

IV. NUMERICAL RESULTS

A. Simulation Results

To compare the performance of the two presented algorithms, a simulation has been carried out with four transmitters (the minimal number of transmitters required by the SI method), one receiver, and one target. The positions of the transmitters are listed in Table I. The target position was $\mathbf{x}_t = [5,5,5]^T$ km. The measurements of the bistatic range were distorted by an additive zero-mean Gaussian error with standard deviation $\sigma_{Ri} = 10$ m, for $i = 1,\ldots,4$.

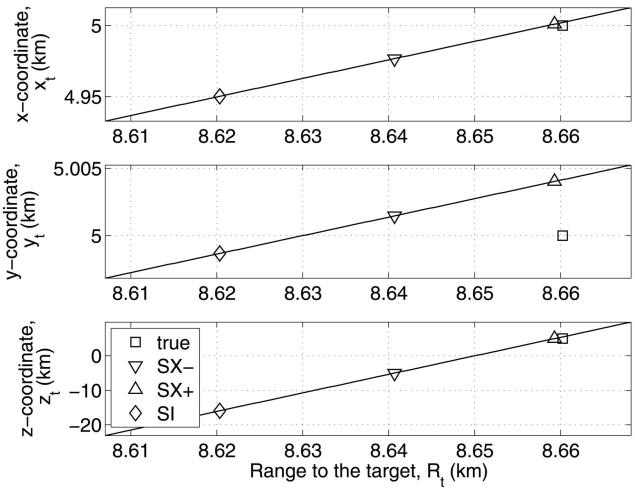

Fig. 2. Target position versus estimated range to target R_t.

Fig. 2 shows the x, y, and z coordinates of the target position calculated according to (12) versus R_t for a single run of the experiment. Since the equation is linear in R_t, the position also changes linearly. The position marked with □ corresponds to the true target position. As can be seen, the true position does not lie on the line because of measurement errors. The positions marked with △ and ▽ correspond to the two roots of the quadratic equation (20), which are the solution of the SX method. The two positions are quite close to each other and to the true position in the x and y coordinates. However, they correspond to two positions symmetrical with respect to the x-y plane—one of positive and the other of negative height. The position calculated with the SI method is marked with ♢. The calculated value of R_t differs slightly from the solutions, obtained with the SX method. This difference has negligible influence on the estimation in the x and y directions (all values are close to the assumed [5,5] km position). However, the incorrect estimation of R_t in the SI method led to an unacceptable error in the z coordinate (the z coordinate was estimated as −18 km in the considered example, as compared with the assumed +5 km).

As was mentioned earlier, the condition that $R_t = \|\hat{\mathbf{x}}_t\|$ has been enforced in the derivation of the SX algorithm, but not in the SI algorithm. The relationship between the range to the target R_t set in (12) and the range to the target calculated from the estimated position $\hat{\mathbf{x}}_t$ is shown in Fig. 3. The horizontal axis corresponds to R_t (which is the independent variable) used in (12) to calculate the target position $\hat{\mathbf{x}}_t$. The vertical axis corresponds to the range to the target calculated as $R_{tc} = \|\hat{\mathbf{x}}_t\|$. The solid line is the curve of calculated range to the target

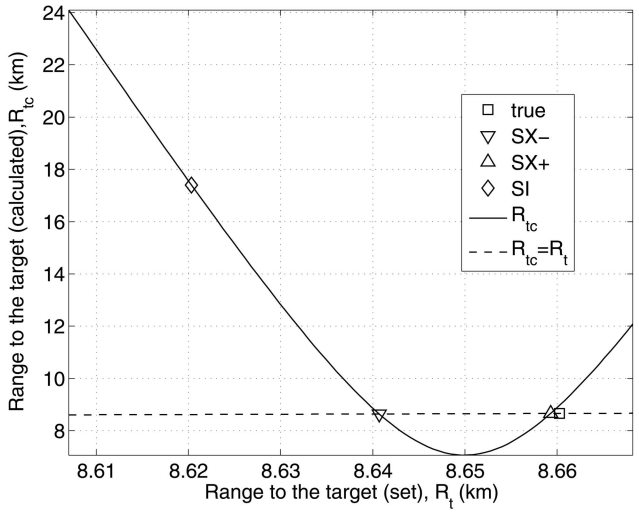

Fig. 3. Calculated range to the target R_{tc} versus set range to target R_t.

R_{tc}. The dashed line is the reference line $R_{tc} = R_t$ (on the plot, this line is almost horizontal due to different scales on the horizontal and vertical axes). The solid line intersects the dashed line at two points, which correspond to the two solutions of the quadratic equation of the SX algorithm (marked with $\triangle$ and $\triangledown$). The solution corresponding to the SI method (marked with $\diamondsuit$) is far away from the dashed line.

This example shows the importance of estimating R_t correctly. The properties of the two algorithms, SI and SX, presented in this example are more general, as confirmed in our statistical experiments. Table II shows the results of 1000 Monte-Carlo simulations of the analyzed scenario. The accuracies calculated for the two algorithms clearly indicate that the SX algorithm outperforms the SI algorithm in this scenario. For this reason, we suggest that the SX method be used in practical applications. This stands in contradiction to the result presented in [12] in the context of TDOA localization, where it was shown that the SI algorithm was better than the SX algorithm. The reason for different results in the TDOA system and passive radar is that the formulation of the problem is different: in TDOA system we operate on differences of ranges, and in passive radar on sums of ranges. Moreover, in the scenario analyzed in [12], closely spaced receivers and a source placed far away were assumed. On the other hand, a typical situation in passive radar involves transmitters (or receivers) distributed over a relatively large area, compared with the distance to the target. An additional advantage of the SX method, apart from better accuracy, is that it can be used in the case of a minimal number of transmitters. Consequently, the SX method is the focus of the remaining part of the paper.

The SX algorithm was tested further by performing a series of Monte-Carlo simulations in a three-transmitter scenario. The scenario was based on the localization of the transmitters and receiver in a real measurement campaign, which is described at the end of this section. The positions of the three transmitters, Pruszkow, Raszyn and Warsaw, are listed in Table III.

TABLE II
Comparison of the Estimation Accuracy

Algorithm	σ_x (m)	σ_y (m)	σ_z (m)
Spherical interpolation (SI)	63.16	13.54	25748.91
Spherical intersection (SX)	6.36	12.28	18.96

TABLE III
Relative Positions of the Transmitters

Transmitter	x-offset (km)	y-offset (km)	z-offset (km)
Tx1 (Pruszkow)	9.63	−2.66	0.20
Tx2 (Raszyn)	19.00	−14.53	0.26
Tx3 (Warsaw)	27.40	3.15	0.22

The simulations were performed over an area of 50×50 km. The altitude of the target was fixed at 10 km. The bistatic measurements were disturbed by an additive zero-mean Gaussian random variable with standard deviation $\sigma_R = 300$ m; this value is typical for an FM-based passive radar. The experiment was repeated 1000 times for each position on the grid. The experimental accuracy was calculated as the standard deviation of the error between the estimated and true parameters. The theoretical accuracy was calculated according to (23). The results regarding the position estimation accuracy are shown in Figs. 4, 5, and 6, for the x, y, and z coordinates, respectively. The accuracy obtained in the experiment (solid line) is similar to the theoretical accuracy (dashed line) for the x and y coordinates. For the z coordinate, however, the theoretical accuracy is calculated accurately only in the vicinity of the transmitters and the receiver. For further ranges, the theoretical predictions are more pessimistic than the actual accuracy. This is due to the fact that from the two solutions of the quadratic equation we select the one with positive altitude, thus, we are using a priori knowledge about the target properties. We are thus censoring the results, which leads to errors lower than predicted by the theory.

B. Real-Life Results

The SX algorithm was tested on real-life data acquired with an experimental passive radar called PaRaDe (passive radar demonstrator) [6, 7] constructed at the Warsaw University of Technology. It is an FM-based system equipped with an 8-element antenna array. In the experiment, a single target was selected at the position $[8.3, 8.4, 2.3]^T$ km. The estimation accuracy was calculated by comparing the results from the passive radar with data provided by a

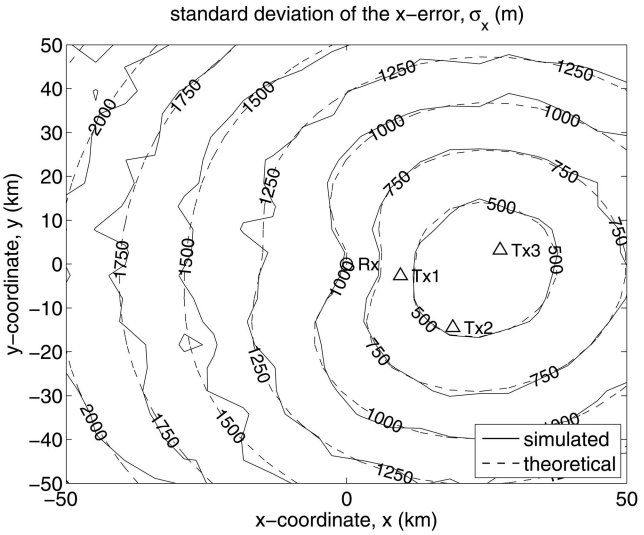

Fig. 4. Simulated (solid line) and theoretical (dashed line) standard deviation of position error in x direction.

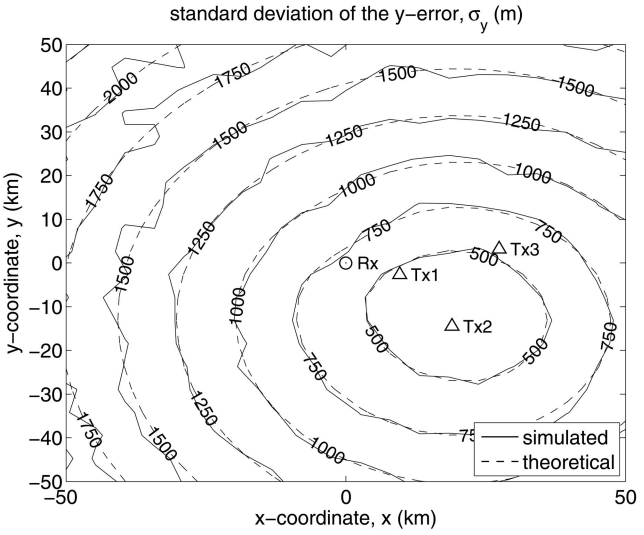

Fig. 5. Simulated (solid line) and theoretical (dashed line) standard deviation of position error in y direction.

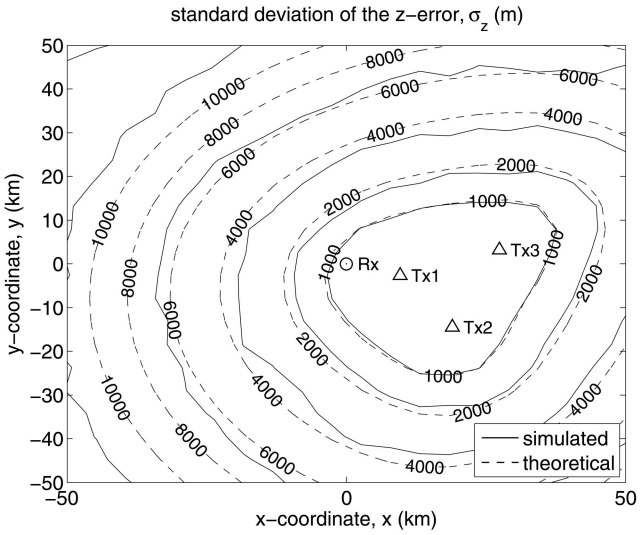

Fig. 6. Simulated (solid line) and theoretical (dashed line) standard deviation of position error in z direction.

TABLE IV
Standard Deviation of the Bistatic Range Errors

Transmitter	σ_{Ri} (m)
Tx1 (Pruszkow)	120
Tx2 (Raszyn)	567
Tx3 (Warsaw)	266

TABLE V
Standard Deviation of the Position Estimation Errors

Standard Deviation	Estimated	Theoretical
σ_x (m)	558	777
σ_y (m)	1248	1388
σ_z (m)	3826	5612

commercially available Mode-S receiver. That allowed us to calculate the estimation accuracy in bistatic coordinates as well as in Cartesian coordinates.

Firstly, the positions obtained from the Mode-S in Cartesian coordinates were converted into bistatic data. These results were compared with the measurements from the passive radar. The standard deviations of the bistatic range measurements corresponding to the three transmitters are listed in Table IV. The bandwidth of the FM radio signal is of the order of tens of kilohertz, which provides range resolution of a few kilometers. However the achievable accuracy of range measurement can be much better, especially for high signal-to-noise ratios. In our example the precise range measurement was carried out by fitting a parabolic curve to the target echo. The range estimate corresponded to the maximum of the fitted parabola. The achievable range resolution is on the order of hundreds of meters, which is an order of magnitude better than the size of the range resolution cell.

Calculations of the standard deviation for the scenario are presented in Table V. It was assumed that the position of the target does not change significantly, so that the accuracy remains fairly constant throughout the experiment. The estimated accuracy was calculated as the standard deviation of the difference between the position from the Mode-S receiver and from the radar in the appropriate direction (x, y or z). The theoretical values of the standard deviation corresponded to the values from the diagonal of the **P** matrix calculated according to (23). The values of σ_{Ri} needed for the calculation of the **P** matrix were taken from Table IV. As the results show, the theoretical results are confirmed by the measurements.

V. CONCLUSIONS

The paper presented two methods for calculating the Cartesian position of a target in a multistatic passive radar. The algorithms were derived based on solutions available for TDOA systems. For the

two algorithms presented, SX outperforms SI in the considered example. For this reason, we recommend the SX method for use in passive radar. This result is contrary to that in the TDOA case, where the SI method performed better [12].

Since both algorithms are based on closed-form equations, they are fast, so they can be easily used in real-life systems, e.g. for track initialization, even in the case of numerous transmitters and targets.

The actual accuracy of the SX method appears close to theoretical results, as suggested by our Monte-Carlo simulations. The algorithm has also been successfully applied to real-life data.

REFERENCES

[1] Friedlander, B.
A passive localization algorithm and its accuracy analysis.
IEEE Journal of Oceanic Engineering, **OE-12**, 1 (Jan. 1987), 234–245.

[2] Herman, S. and Moulin, P.
A particle filtering approach to FM-band passive radar tracking and automatic target recognition.
In *Proceedings of the IEEE Aerospace Conference 2002*, vol. 4, 2002, 4-1789–4-1808.

[3] Howland, P.
Target tracking using television-based bistatic radar.
IEE Proceedings—Radar, Sonar and Navigation, **146**, 3 (June 1999), 166–174.

[4] Howland, P., Maksimiuk, D., and Reitsma, G.
FM radio based bistatic radar.
IEE Proceedings—Radar, Sonar and Navigation, **152**, 3 (June 2005), 107–115.

[5] Malanowski, M.
An algorithm for 3D target localization from passive radar measurements.
In *Proceedings of SPIE—Photonics Applications in Astronomy, Communications, Industry, and High-Energy Physics Experiments 2009*, vol. 7502, Wilga, Poland, May 25–31, 2009, 75 021B-1–75 021B-6.

[6] Malanowski, M., Kulpa, K., and Misiurewicz, J.
PaRaDe—Passive radar demonstrator family development at Warsaw University of Technology.
In *Proceedings of the Microwaves, Radar and Remote Sensing Symposium*, Kiev, Ukraine, Sept. 22–24, 2008, 75–78.

[7] Malanowski, M., et al.
FM based PCL radar demonstrator.
In *Proceedings of the International Radar Symposium 2007*, Cologne, Germany, Sept. 5–7, 2007, 431–435.

[8] Mellen, II, G., Pachter, M., and Raquet, J.
Closed-form solution for determining emitter location using time difference of arrival measurements.
IEEE Transactions on Aerospace and Electronic Systems, **39**, 3 (July 2003).

[9] Nordwall, B. D.
'Silent Sentry' a new type of radar.
Aviation Week and Space Technology, 30 (1998), 70–71.

[10] Schau, H. and Robinson, A.
Passive source localization employing intersecting spherical surfaces from time-of-arrival differences.
IEEE Transactions on Acoustics, Speech, and Signal Processing, **ASSP-35**, 8 (Aug. 1987), 1223–1225.

[11] Schmidt, R.
A new approach to geometry of range difference location.
IEEE Transactions on Aerospace and Electronic Systems, **AES-8**, 6 (Nov. 1972), 821–835.

[12] Smith, J. and Abel, J.
Closed-form least-squares source location estimation from range-difference measurements.
IEEE Transactions on Acoustics, Speech, and Signal Processing, **ASSP-35**, 12 (Dec. 1987), 1661–1669.

[13] Smith, J. and Abel, J.
The spherical interpolation method of source localization.
IEEE Journal of Oceanic Engineering, **OE-12**, 1 (Jan. 1987), 246–252.

[14] Tan, D., et al.
Passive radar using Global System for Mobile communication signal: Theory, implementation and measurements.
IEE Proceedings—Radar, Sonar and Navigation, **152**, 3 (June 2005), 116–123.

[15] Tobias, M. and Lanterman, A. D.
Probability hypothesis density-based multitarget tracking with bistatic range and Doppler observations.
IEE Proceedings—Radar, Sonar and Navigation, **152**, 3 (June 2005), 195–205.

Mateusz Malanowski (S'02—M'08) received his M.S. and Ph.D. degrees in electronics from the Warsaw University of Technology, Warsaw, Poland, in 2004 and 2009, respectively.

He was a research scientist with FGAN (Forschungsgesellschaft fuer Angewandte Naturwissenschaften), Germany, and an Engineer with Orpal, Poland. Currently, he is an assistant professor at the Warsaw University of Technology. His research interests are radar signal processing, target tracking, passive coherent location, synthetic aperture radar and noise radar.

Dr. Malanowski is the author/coauthor of over 50 scientific papers. He is a member of the Institution of Engineering and Technology (IET).

Krzysztof Kulpa (M'91—SM'10) received his M.S., Ph.D., and D.Sc. degrees in electronics from the Warsaw University of Technology, Warsaw, Poland, in 1982, 1987, and 2009, respectively.

He is presently an associate professor at the Warsaw University of Technology and the Head of Signal Processing Laboratory. Prior to that he was an assistant professor at the Technical University of Bialystok (1988–1990). Between 1990 and 2005, he was a scientific advisor in RADWAR S.A. His research interests are radar signal and data processing including detection, tracking, passive coherent location, synthetic aperture radar, inverse synthetic aperture radar and noise radar.

Dr. Kulpa is the author/coauthor of over 200 scientific papers. He is a member of the Institution of Engineering and Technology (IET). He was a Chairman of the Polish chapter of the IEEE Signal Processing Society (2003–2005), a program committee member of several radar conference series, such as International Radar Symposium (2004–2010), European Conference on Synthetic Aperture Radar (2002–2010), European Radar Conference (2007–2010), International Conference on Information Fusion (2006–2010) and others, and the initiator of the Signal Processing Symposium conference series.